July 2018

Isoperibolic Hydrogen Hot Tube Reactor Studies

FINAL PROGRESS REPORT

FOR THE PERIOD JULY 1ST 2016 THROUGH JULY 31ST 2018

SRI International Project P21429

Prepared by:
Francis Tanzella, Principal Investigator, Manager
Low Energy Reactions Research Program
Energy and Environment Center
Advanced Technology and Systems Division
SRI International
Menlo Park, California

Sponsored by:
Brillouin Energy Corporation
Berkeley, California

Attention:
Mr. Bob George II, Chief Executive Officer
Mr. Robert Godes, Chief Technology Officer
Mr. David Firshein, Chief Financial Officer

Table of Contents

EXECUTIVE SUMMARY

Introduction

In August 2012, SRI International (SRI - https://www.sri.com) was contracted by Brillouin Energy Corp. of Berkeley California (BEC– http://brillouinenergy.com) to perform independent studies of Brillouin's low energy nuclear reaction (LENR) reactors, as well as advise on related Brillouin LENR research. We have operated these reactors to observe, monitor, analyze, advise on, and independently verify Brillouin's LENR evolving research & development work, test systems, and test results. This Report documents the independent results obtained with Brillouin's prototype isoperibolic reactors located in SRI's laboratory, as well as verification and validation of results obtained with Brillouin's prototype isoperibolic reactors located in Brillouin's laboratory, over the term of this contract. Brillouin indicates that it has designed the control systems in its reactors to drive the underlying physics of LENR, as described in its Controlled Electron Capture Reaction (CECR) Hypothesis, which is how it believes its reactors generate controlled LENR Reaction Heat. This Report does not attempt to prove or disprove Brillouin's CECR Hypothesis. This report will emphasize the results obtained during the first 7 months of 2018, introductory material, background material, and results summary covering the whole term of this effort, which are repeated for clarity.

The systems tested and described in this report consist of three parts – reactive tubes, reactors and calorimeters. The tubes are the reactive components of the system. (Brillouin energy is engineering the system with the intent of licensing production and the tube design allows any tube to operate in any similarly sized reactor). The reactors provide the environment and stimulation that causes the tubes to produce LENR reaction heat. The calorimeter is used to measure the thermal efficiency and absolute heat produced by the tube, and/or the reactor. The calorimeter was designed by both SRI and Brillouin personnel to be perfectly matched to the reactor for accuracy of measurement, whose results are described in this report. In 2017 the calorimeter design was modified to match the analytical methodology suggested by an independent commercial third-party reviewer, who is also overseeing their suggested stimulation and analyses (see dynamic stimulation below).

SRI has brought over 75 person-years of calorimeter design, operation, and analysis experience to this process. We have used our expertise in LENR calorimetry, the ability to measure input and output power in the form of electricity or heat (energy balance power gain), to validate the results that are summarized in this Technical Progress Report. Brillouin's system was designed to rely upon compensation calorimetry, which is an accepted method of examining the variables that affect power gains.

This Technical Progress Report is the third such report that SRI International has issued to Brillouin Energy Corp., covering technical results achieved from July 2016 through 2018 and serves as the project's Final Report.

Experimental

Since the start of SRI's independent advisory and independent experimental verification and validation role in August 2012, to date Brillouin has developed its uniquely fabricated, hydrogen

"gas-based" reactors, known as its "Hydrogen Hot Tube" (HHT[tm]), in order to prove that its CECR Hypothesis can generate controlled LENR heat on demand for potential industrially useful applications. During this time, Brillouin has run many experiments at its headquarters lab in Berkeley, as have SRI personnel at SRI in Menlo Park. These results have produced, at various times, a wide range of thermal output, which can be attributed to LENR Reaction Heat in Brillouin's HHT[tm] prototype reactor test systems.

SRI has aided in the evaluation of the effectiveness of the two gas mass flow calorimeters used with Brillouin's first generation (GEN1) HHT[tm] reactor using "ConFlat®" fittings. SRI has also been instrumental in the subsequent design & development of the isoperibolic calorimeter ("IPB" - see Theory of Isoperibol Calorimetry, E.D. West, Journal of Applied Physics 41, 2705 (1970); https://goo.gl/6Rc11x) used to measure and validate the energy balance of Brillouin's second generation IPB HHT[tm] reactors (GEN2). Brillouin has built, calibrated and tested four identical IPB systems at Brillouin's lab. Two IPB HHT[tm] reactors are now operating in Brillouin's laboratory and two were operating at SRI during the final 18 months of this project. Tubes have been transferred and operated successfully within the IPB HHT[tm] reactors at SRI after operating successfully within the IPB HHT[tm] reactors in Brillouin's facility, and one such is described in this report. Because of their highly refined calorimetry, both Brillouin and SRI have concentrated on the extensive testing of these (GEN2) IPB HHT[tm] reactors:
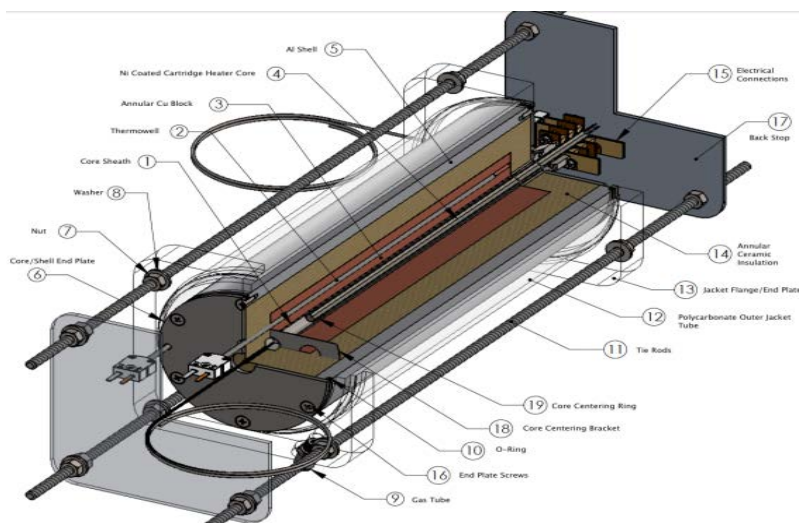
Schematic diagram of the isoperibolic hydrogen hot tube reactor/calorimeter

The design of the Brillouin IPB HHT[tm] includes a conventional resistive heater used to maintain a constant temperature in the reactor while adding additional proprietary electrical "Q" pulses to the system to stimulate the specially designed tube to yield LENR heat. This becomes evident if the total output heat measured is greater than that from the heater and the Q-pulse power imparted to the tube. Upon generating a positive LENR coefficient (excess heat), the system reduces the heater power input, by an amount equal to the Q pulse power imparted to the tube and the excess power generated, required to maintain the pre-set temperature. By this compensation calorimetry method, the measurements of net input and output power are carefully measured to within 5% accuracy to assure an exact calculation of the LENR coefficient.

SRI has closely followed and advised on the evolution of Brillouin's system design and materials and as such we are very familiar with the history of their efforts to build and advance their test systems, test protocols, manufacturing techniques, specifications and tube components. We closely studied Brillouin's test data generated from extensive testing of their IPB HHTs during the term of this report.

Results

We report here on the overall extensive testing of the four IPB HHT^tm reactors operating at both Brillouin and SRI. Together we have tested 56 tubes during the term of this contract (23 tubes in two reactors at SRI and 33 tubes in two reactors at Brilouin).

In 2017, we were able to again corroborate that the Brillouin IPB HHT^tm system that was moved to SRI continued to produce similar LENR Reaction Heat that it produced up in its Berkeley laboratory at Brillouin. Together with our prior data review, it is now clear that these very similar results are independent of any of these systems' location (Berkeley or Menlo Park) or operator (Brillouin's or SRI's personnel). This transportable and reproducible reactor system is extremely important and quite rare. These two characteristics, coupled with the ability to start and stop the reaction at will are, to our knowledge, unique in the LENR field to date.

2017's Report showed that such LENR reaction output had increased to as much as over five watts of power, on a fully controlled basis, on demand.

Brillouin has posited that this specific heat production is being generated from its CECR process, based on its interpretation of the precise calorimetric measurements of the input and output power in its IPB HHTs. The current results also suggest that the tubes in three different IPB HHTs produced similar LENR heat outputs, using two different stimulation/analysis methods, and using different tube materials (key components). In addition, an IPB tube showing reaction heat has been was removed from service at BEC during December 2017 and was placed in service at SRI in a different reactor during April 2018 and showed similar results.

Using different batches of the same materials and standard industrial processing techniques, processed to a proprietary set of customized specifications, Brillouin has produced a variety of similar tubes for its HHT^tm systems. This was done in order to test various materials and their fabrication techniques, which yield different material and electrical properties necessary to maximize the effect of the Q pulse.

We have used different methods of stimulation, each requiring its own analysis method. These are explained in more detail in the body of this Report. The "steady-state method" was used extensively during the earlier years of this project. The "dynamic method", used more recently, provides a more precise and accurate analysis but is not directly comparable to the results found using the "steady-state method". Earlier we calculated the coefficient of performance (COP) by dividing the tube's output power gain by the input pulse power. If we interrupt the dynamic stimulation to yield a steady-state, we can divide the tube's apparent power gain by the input pulse power and compare the two methods' results. The results of a dynamic stimulation with a corresponding legacy-type analysis from recent runs are shown next in Table E.1:

Table E.1 Coefficients of performance (COP) from recent runs using legacy analysis method

Temperature/°C	$Q_{REACTION}$/Watts	COP
300	3.62	1.56
340	2.71	1.37
300	3.59	1.55
340	3.22	1.43
300	3.90	1.62
340	3.58	1.44
300	4.91	1.56
340	5.29	1.52
300	4.99	1.58
340	5.35	1.53
300	4.85	1.58

In our extensive review of the test data generated from all four of Brillouin's IPB HHT^{tm} systems, from test runs made at both SRI's laboratory and Brillouin's laboratory during this project, the test data showed and continues to show that LENR heat outputs of several watts were repeatedly produced from positive coefficients in the range of 1.2X to 1.6X, depending on various factors, including the analysis method, We feel that the calorimetry was studied exhaustively and validated to an extremely high level of accuracy (see further discussion and test data review below).

As tube engineering and manufacturing continues to improve, and more protocols and parameters are tested and refined, we expect to see more of the higher COP's. When the legacy-type analysis method similar to that used earlier is used to calculate the COP from the dynamic stimulation runs, we get significantly larger COP's than those measured earlier. It is also important to note that the absolute LENR power outputs are significantly larger than those that were measured earlier.

The most impressive result was when an active tube, which gave the best results last year was removed from service at BEC during December 2017, and was placed in service at SRI in a different reactor during April 2018 it showed similar results.

Conclusions

The LENR coefficients of performance (COPs) that have been produced in the Brillouin IPB HHTs recently, and the related power output levels of several watts are small-scale but obviously greater than those produced earlier. Further, the consistent repeatability of their tubes' production, together with ongoing refinement of their manufacturing techniques, specifications, and components, have led to independently verified repeatable results, unprecedented in the field. The transportability of the system, as documented the 2016 Report, and reproduced in 2018, is also a considerable achievement. While these achievements are still being produced in a test laboratory at bench scale, they are pointing at an engineering pathway toward a future commercial design. To the best of our knowledge, these results are unique in the LENR field of study at this time.

Importantly the results presented here, although modeled in a way to account for all input and output powers, do not use all of the heater power necessary to maintain temperature and the losses in the pulse generator, to calculate the COP. Brillouin engineers are confident that these power losses can be minimized or eliminated in future designs with conventional engineering efforts. This is an ongoing issue that will have to be addressed in order to scale these results to a commercial level. Nonetheless:

These latest results continue to demonstrate that:

♦ The repeatability and the consistency of the system output are similar, regardless of in which reactor that any particular tube is tested and which tube components of a given design are being used, interchangeably.
♦ To our knowledge, this ability to demonstrate the production of a verifiable and repeatable LENR heat output with positive COPs, which are consistently initiated and uninitiated on command using system design control mechanisms are unique in this field.
♦ As documented again recently, Brillouin has invented and built LENR reactor systems that have been shown to be transportable from its own laboratory while showing the same positive results in a new laboratory. In 2017, a second Brillouin IPB HHT^{tm} prototype unit was transported from the Brillouin laboratory to SRI, for purposes of independent operation, verification, and validation. Both reactor units at SRI produced, and one continues to produce, excess power as did the other two reactor units in Berkeley.
♦ Significant progress in increasing the COP, and the absolute LENR reaction power output in total watts, was made over the term of this project.

Correlation of different fabrication materials and methods as well as various electronic measurements with measured COPs have shown which methods are more successful and allow us to design reactor tubes more likely to yield higher COPs as this work continues. These results are given in the Confidential Client Private Addendum.

In summary, when using tubes constructed from similar metal compositions and built to the same industrial specifications, the Brillouin IPB HHT^{tm} LENR prototype reactors continue to show results that are potentially:

- Controllable on demand
- Reproducible
- Transportable
- Generated from multiple system components, made from relatively identical compositions, manufactured to the same industrial specifications, producing the same LENR heat output results
- Generating significantly greater, repeatable COP's and absolute LENR power outputs as the project progressed.

Side note: The above positive COP results were produced at operating temperatures of between 300°C to 340°C. The ultimate operating temperature of an HHT commercial system is primarily related to the COP produced, and other engineering factors, and is not in itself a limiting factor per se. Brillouin has had success using similar reactors

and tubes operating at up to 700°C, which is a much more desirable operating range for the commercial HHT systems that Brillouin anticipates building in the future as it continues its efforts to scale its development.

INTRODUCTION

Since August 2012, SRI has been performing tests on two different versions of Brillouin Energy Corp.'s low energy nuclear reactors (LENR) under SRI project P21429. We have operated these reactors to independently attempt to verify results that Brillouin has found with these reactors and other type of reactors. We have also monitored and advised Brillouin on the results found in reactors operated by Brillouin in their own laboratory. This Report documents the results obtained by studies in SRI's laboratory, as well as verification and validation of important results obtained in Brillouin's laboratory during the term of this project. Brillouin has indicated that it has designed the control systems in its reactors to drive the underlying physics of LENR, as described in its Controlled Electron Capture Reaction (CECR) Hypothesis, which is how it believes its reactors generate controlled LENR Reaction Heat. This study did not attempt to prove or disprove Brillouin's Controlled Electron Capture Reaction (CECR) Hypothesis.

The systems tested and described in this Report consist of three parts – tubes, reactors and calorimeters. The tubes are the reactive components of the system. The reactors provide the environment and stimulation that causes the tubes to produce reaction heat. The calorimeter is used to measure the thermal efficiency and absolute values of electrical power input to versus heat or thermal power output from the tube-reactor system. The calorimeter used in recent years was designed by both SRI and Brillouin personnel to be perfectly matched to the reactor, whose results are described in this Report. This report will concentrate on the isoperbolic (IPB) reactor/calorimeter type of experiments, as these represent the most important work performed in the recent 3 calendar years.

SRI has brought over 75 person-years of calorimeter design, operation, and analysis experience to this process. We have used our expertise in low energy nuclear reaction (LENR) calorimetry – the ability to measure input and output power in the form of electricity or heat (energy balance power gain), to validate the results that are summarized in this Report. Brillouin's system design utilizes compensation calorimetry, where the tube and reference temperatures are held constant by varying the input heater power while applying different types of stimulation, which also input power to the reactor/calorimeter. In 2017 the Brillouin Energy team started working with an independent commercial third party to develop a thermal model based on heat input and loss identification. This "dynamic" method of analysis allows us to analyze all power entering or affecting the tube as well as all power emanating from the tube based on differential equations describing temperatures and power measurements. While this requires 100 hours of calibration and up to 40 hours of excitation to verify a calibration, it allows testing of 12 parameter variations per hour versus one or two in the traditional steady-state method.

EXPERIMENTAL

DESIGN

The tubes consist of a substrate, which in some configurations includes a heater and thermocouple, with several spray-coated layers. Generally, these coatings alternate between a hydrogen-absorbing metal and an insulating ceramic. One example is shown in Figure 1. Other designs may have more or less layers. All of the layers are porous, allowing the gas(es) in the reactor chamber access to all coatings. In some experiments, there is a heater and thermocouple in the center of the tube. In other runs the heater is inserted into or attached to the inner block, as explained below. The power to the heater is measured directly from the voltage and current supplied by the direct current (DC) power supply.

Several different types of IPB tube/reactor systems were used during this project. In the early experiments we used stainless steel tubes with a coat of alumina sprayed on top before being coated with the $Ni/Al_2O_3/Ni$ "sandwich". Then tubes built up on top of a cartridge heater with a built-in thermocouple. In the latest design, the inner block thermocouples were imbedded in the middle of the block. With this design, essentially all of the heater power was imparted into the tube. Later the tube heater system was replaced with two band heaters wrapped around the outside of the inner block, directly over the center six inches of the tube. In this design, one inner block thermocouple was held directly under one band heater while the other was strapped to the outside of the block toward an axial end of the block. In this latter design, only a fraction of the heater power is imparted into the tube since a significant fraction is lost to the cooling fluid.
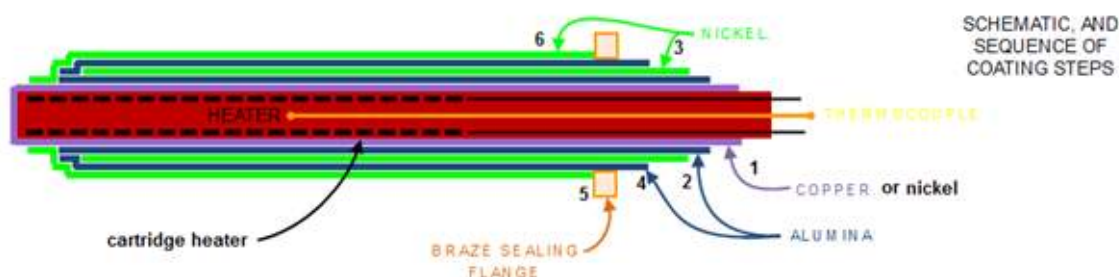

Figure 1. Example of Brillouin's fourth generation Hydrogen Hot Tube Tubes

A photograph of the reactor/calorimeter system is shown in Figure 2. The system is contained in an acrylic container filled with argon gas, which serves several functions. The first function is to minimize the probability of a hydrogen-oxygen reaction from any H_2 that might leak from the system. The second function is to keep the inside of the reactor from oxidizing. The third function is to control the conduction of heat between the sections of the calorimeter. A schematic diagram of the reactor/calorimeter system is shown in Figure 3.
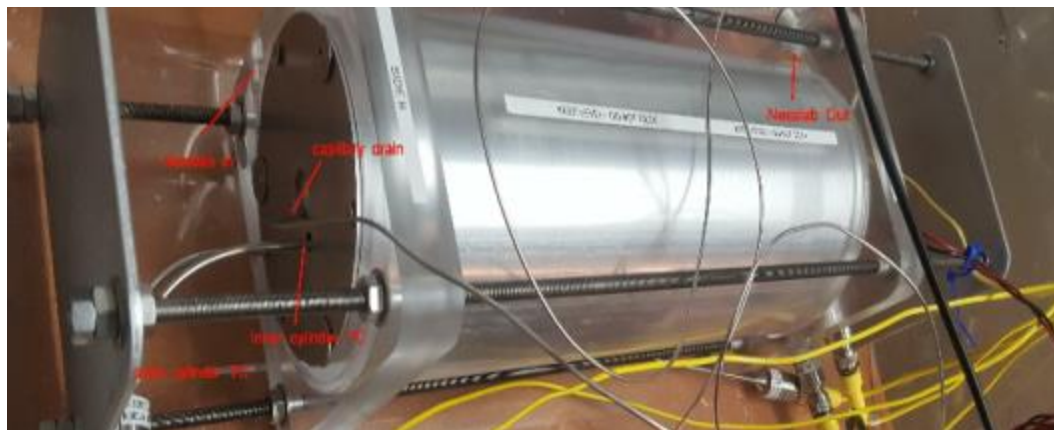
Figure 2. Photograph of the reactor/calorimeter system

In a traditional isoperibolic calorimeter, the reactor temperature is distributed along a massive thermal block (inner block) surrounded completely by a thick insulating layer, which itself is surrounded by another thermally conductive metal mass (outer block). This latter block is kept at a constant reference temperature.
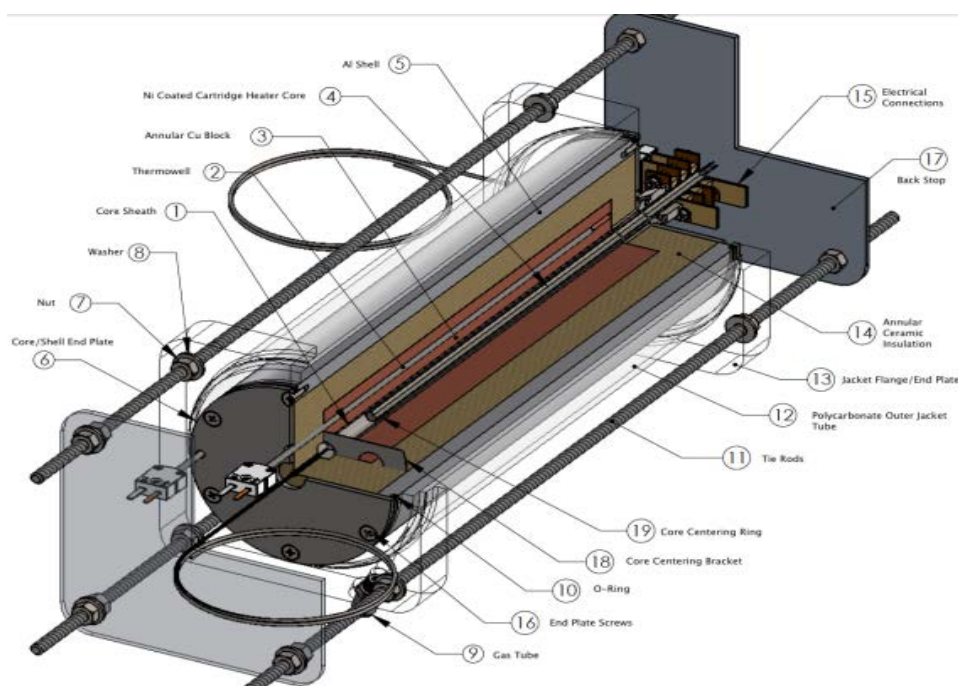

Figure 3. Schematic diagram of the isoperibolic hydrogen hot tube reactor/calorimeter

Referring to the labeled parts of Figure 3, the tube (4) is centered in and insulated from a metal sheath (1). This tube/sheath combination together with the electrical connections (15) comprise the reactor. An annular steel block (3) is in intimate contact with the reactor sheath and contains a thermowell, (2) and thermocouples and acts as the inner block. Either a cartridge heater was

inserted into this block or band heaters were clamped to the block. This steel block is surrounded by an annular ceramic insulator (14). Argon gas is used to purge this insulated chamber. Surrounding this insulator is an aluminum shell (5) with thermowell and thermocouples. This shell, kept at constant temperature by flowing temperature-controlled water between it and the outer acrylic sleeve (12), serves as the outer block. Argon gas is circulated through the insulated chamber outside of the calorimeter.

A description of the various tubes used are documented in Appendix A.

MEASUREMENT

The outer active layer of the tube is stimulated by sending pulses through the outer layer or layers and returning electrically through the innermost layer. The nature of the pulses is such that its current travels primarily on the surface of the metal in contact with the ceramic (the "skin effect"). This effect is caused by the conductivity and magnetic permeability of the metal and initiated by the very fast rise time of the pulses, similar to that seen with very high frequency sine or square waves. An example of this pulse design, which Brillouin refers to as a "Q Pulse", is shown in Figure 4. The pulse width is now from ~30 – 10,000ns with a duty cycle normally of less than 1%. More detail on the pulse trains are shown in an issued patent[1].
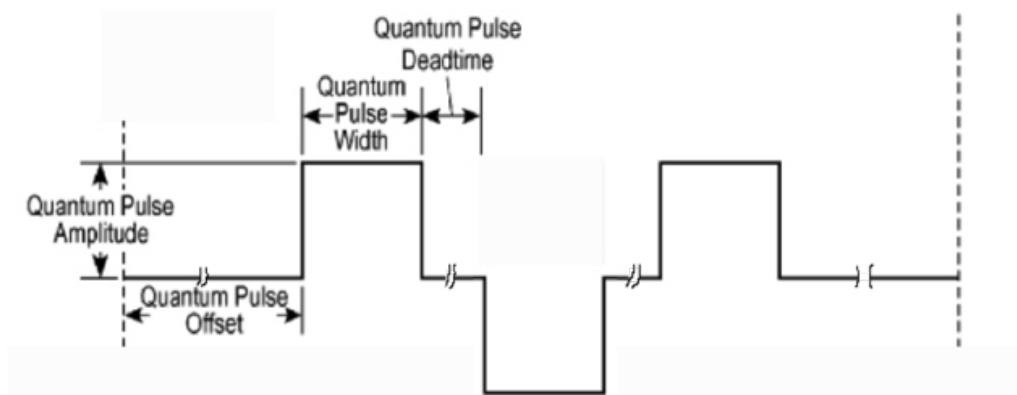

Figure 4. Example of Brillouin's "Q Pulse".

The stimulation power imparted to the tube is measured using a circuit shown in Figure 5. The pulse is generated by a proprietary Q Pulse board and delivered to the tube using a termination resistor in series, which helps match the load impedance to that of the pulse board output. Using a high-speed oscilloscope, the voltage across the end of the tube nearest the pulse board is measured as well as the voltage across the opposite end of the tube including the termination resistor (Zterm). Zterm also acts as a current measuring resistor. The root mean square (rms) voltage across Zterm is then converted to the rms current.
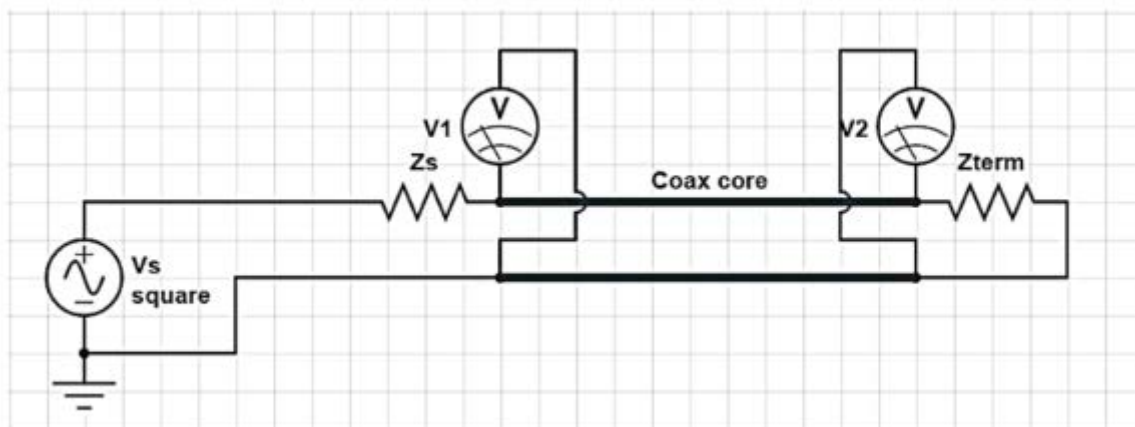
Figure 5. Pulse power measurement circuit

The power imparted to the tube is determined using the voltage red and blue traces shown in Figure 6. The difference between the two voltage traces, is calculated after aligning them in a way that minimizes the time difference. This overestimates the power imparted to the tube by a small amount since any phase lag between voltage and current would impart less input power. The current calculated from V_2 is shown in black and the product of it with the voltage difference (power) is shown in green. It has been shown that the power calculation is essentially the same (within measurement error) whether it is calculated by multiplying the current and voltage plots point by point or by multiplying the calculated rms voltage by the rms current.
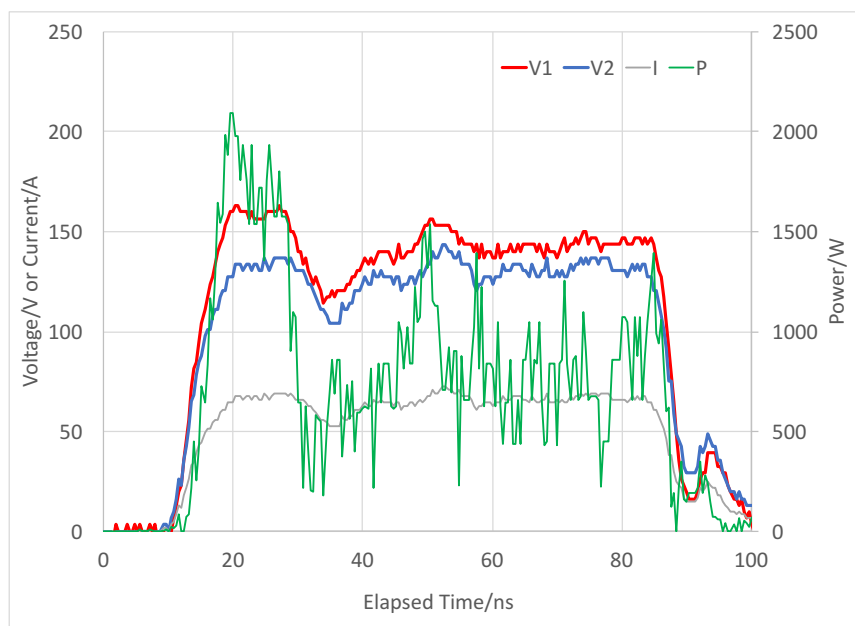

Figure 6. Measurement of the Q-pulse power across the tube

In compensation calorimetry the heater power is varied to keep either the tube or inner block at constant temperature, which generally also keeps the other at a constant, but slightly different,

temperature. The difference between the heater power with and without stimulation determines the effect of the stimulation. If this difference is greater than the stimulation that reaches the tube, then energy is being produced in the tube. Approximately 50 different parameters are collected allowing for calculation of Reaction Power (the power produced by the process induced by the pulse stimulation). Several calculation methods are possible from these parameters. In addition, two different stimulation sequences are used. In the Analysis section we describe these two sequences and the calorimetry method used for each of them.

OPERATION

Figure 7 shows a screenshot from the specially-designed proprietary automation and data collection computer program used to control and collect results from the IPB reactor/calorimeter system. The program has several panes allowing for control of temperature, pressure, pulse voltage, pulse power, pulse width, and pulse repetition rate and gas composition. The program also collects the heater power, the pulse power at the generator as well as at the tube, all temperatures, water flow rates and gas pressure. Hydrogen and oxygen concentrations in the argon blanket are also measured and collected. In all, approximately 50 different parameters are collected and stored every 10 seconds. As mentioned above, a sequence file can be used to automatically change any or all of the input parameters at specified intervals over a multi-day or multi-week period.

The sheath containing the tube is operated with a static fill of hydrogen, helium, or argon gas held at constant pressure up to 10 bar. The temperature of the tube is held constant using whichever heater is installed, and controlled from 200°C to 600°C. The outer block temperature is held at 25°C by constant temperature water flowing from a Neslab® chiller.
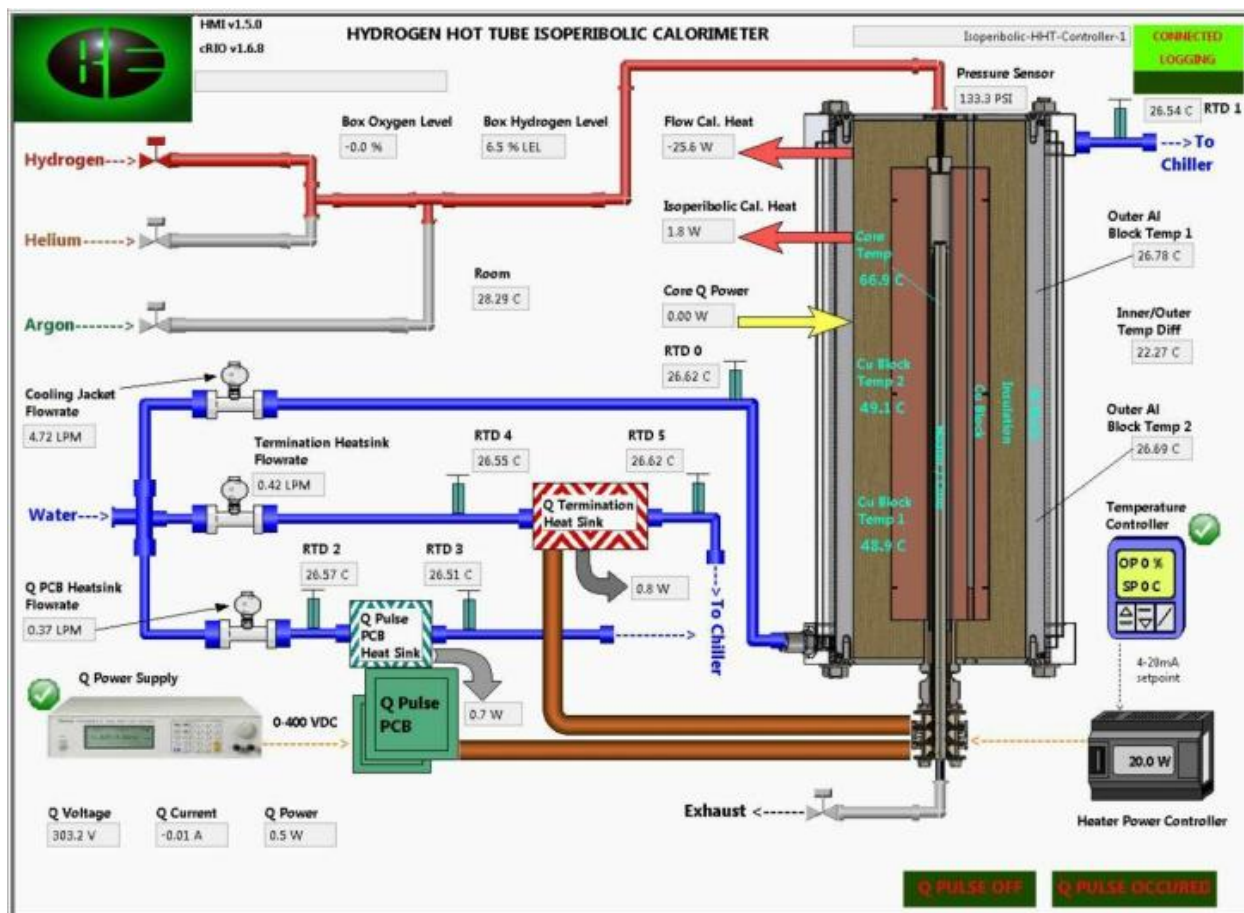
Figure 7. Screenshot of the automation and data acquisition computer program in operation

The power emanating from the Q-pulse generator board, or that applied directly to the tube, is held constant as chosen by the program's front panel or the sequence file. Generally, the pulse amplitude (voltage) and pulse width are chosen. The repetition rate is adjusted automatically to maintain the chosen pulse power. Only a minor fraction of this power from the generator board reaches the tube as most of it is lost as heat in the termination resistor. This is necessary to get an accurate measure of energy actually dissipated in the tube and to match the load impedance to that of the generator thus preventing the pulse from damaging the electronic components. Of that reduced power only a portion of it influences the heater power as explained in the "Measurement" subsection above. The actual pulse power is measured directly via the methodology presented above.

During this project several stimulation methods were tried to find one that can act as a blank (no excess power) using similar Core Q Power. The DC resistive heating of the tube surface coat, was used occasionally and required changing electrical connections and using measurement hardware different from that used for the real-time Core Q Power calculation. Ideally these methods need to be compatible with the data collection's software's calculation designed for the low duty cycle Q pulse square waves and not require hardware changes. Some of the methods tried were: (1) straight sine waves; (2) low duty cycle square waves; (3) large pulse widths with long rise times. Ultimately, calibration runs used Q pulse parameters that were known not to

produce LENR heat (low voltage pulses) but impart the same power to the tube as parameters expected to show LENR heat (high voltage pulses). The hardware was modified to allow pulsing at much higher repetition rates.

First operating in He gas, a sequence was operated from 200°C to 600°C in 50°C intervals. At each temperature a given DC power was applied to the coating on the core. This process was then repeated but applying constant power pulses varying pulse width at each temperature. lastly, both automated sequences were repeated in hydrogen gas

Later were two major methods of operation employed, each requiring a different analysis method. The first method operated with the reactor at a steady-state temperature and input powers, which we refer to as the steady-state stimulation (SSS) method. In our second approach, the dynamic stimulation (DS) method, the heater power was ramped smoothly through a maximum and back down while smoothly ramping Q power up and down several times. The DS method was developed to allow for many Q pulse parameters to be tested in less time. On occasion we would interrupt the DS to allow the system to achieve a steady-state for several hours.

The steady-state stimulation (SSS) method was operated in power compensation mode, where the computer kept the temperature constant at either the tube or the inner block. When power was imparted from the Q-pulse, the heater power was reduced to compensate and maintain a constant temperature. Hence, when the inner and outer block temperatures are held constant, the tube temperature will respond to the stimulation. The output power (calculated from the inner minus outer block temperatures) did not change as the input power compensates for the total power emanating from the tube. The total tube power included the stimulation power and the power due to reaction heat (*i.e.* LENR power).

ANALYSIS

Various tube designs were also implemented. One particular change that affected the calorimetry was applying the active metal coating (Ni or Pd/Ni) over only the middle 6 inches of the tube instead of over the whole portion of the tube inside the calorimeter. In this design, essentially 100% of the Q pulse power imparted to the tube influenced the tube thermocouple's measurement. This is true because only a few percent of the measured Q power was imparted to the very highly conductive Cu coating, which acted as leads to the active metal. When using the earlier design with the active metal running almost the whole length of the tube only a fraction of the imparted tube power was seen by the tube thermocouple and hence compensated for by the heater. As the designs changed so did the measurement and analysis methods.

Method A
In the early IPB design only a fraction of the stimulation power is imparted to the core heater control because the heater/thermocouple combination is only in contact with approximately half of the core's length. The actual fraction imparted to the core is determined by resistively heating the core's coatings using different powers sourced from a well-measured DC power supply and measuring the heater's response at different temperatures. At each temperature, a linear function

(P$_{drop}$ = m*P$_{coating}$ + b) is determined between the power imparted to the core's coating via resistive heating and the power reduction in the internal heater necessary to maintain temperature. Representative linear coefficients at different temperatures are shown in Table 2.

Table 2. Correlation of power imparted to the core's internal heater by resistively heating its coating:
(P$_{drop}$ = m*P$_{coating}$ + b)

Temperature/°C	m	b
150	0.41	0.07
200	0.44	0.10
250	0.48	0.07
300	0.51	0.06
350	0.55	0.01
400	0.56	0.03
450	0.57	0.03
500	0.57	0.07

The basic calorimetric calculations are shown in Equations 1 through 4 when the isoperibolic calorimeter operates in heat flow mode. Heat flow (Q_{flow}) is measured using k_{flow}, which is determined via calibration and the temperature difference between the inner and outer blocks. Heat loss (Q_{loss}) represents the heat loss to air that is not accounted for in (Q_{flow}) and is also determined via calibration. The output heat (Q_{out}) is the sum of (Q_{flow}) and (Q_{loss}). The input heat is the sum of power applied to the heater (Q_{heater}) and the amount of heat experienced by the heater from the pulse (Q_{pulse}). Hence the heat due to the reaction ($Q_{reaction}$) is the difference between the output and input heats.

$$Q_{reaction} = (Q_{flow} + Q_{loss}) - (Q_{heater} + Q_{pulse}) \qquad \text{Equation 1}$$

$$Q_{flow} = k_{flow}(T_{core} - T_{outer}) \qquad \text{Equation 2}$$

$$Q_{loss} = k_{los}(T_{core} - T_{air}) \qquad \text{Equation 3}$$

$$Q_{out} = Q_{flow} + Q_{loss} \qquad \text{Equation 4}$$

We use the subscripts 1 to mean operation without Q power and 2 to mean operation with Q power. In power compensation mode, we compare the heater power imparted to the core with and without Q pulses applied. Because T_{core}, T_{outer}, T_{air} are held constant in this mode Q_{flow} and Q_{loss} are the same with and without Q power. As such Equation 4 cannot be used to calculate Q_{out} in power compensation mode. The difference between $Q_{reaction1}$ and $Q_{reaction2}$ is shown in Equation 5. When Q pulses are not applied Equation 6 defines Q_{pulse} and $Q_{reaction}$ to be zero. This simplifies equation 5 to that shown in Equation 7 where ΔQ_{heater} is the difference between the heater applied with and without Q pulses and ΔQ_{out} is output power with and without Q power. The empirical determination of ΔQ_{out} is shown in Equations 8 through 10.

$$Q_{reaction2} - Q_{reaction1} = (Q_{flow2} - Q_{flow1}) + (Q_{loss2} - Q_{loss1}) -$$

$$(Q_{heater2} - Q_{heater1}) - (Q_{pulse2} - Q_{pulse1}) \qquad\qquad \text{Equation 5}$$

Without Q pulse: $\qquad Q_{pulse1} = Q_{reaction1} = 0\,W \qquad\qquad$ Equation 6

$$Q_{reaction} = (Q_{heater1} - Q_{heater2}) - Q_{pulse} + (Q_{out2} - Q_{out1})$$
$$= \Delta Q_{heater} - Q_{pulse} + \Delta Q_{out} \qquad\qquad \text{Equation 7}$$

Replacing pulses with DC power through the core to emulate the physical source of the heat, as described in the measurement subsection, allows us to determine the amount of Q pulse power that affects the core heater power when $Q_{reaction} = 0$. Rearranging Equation 7 where $Q_{heaterDC}$ is the heater power when DC power is applied to the core coating, Equation 8 allows us to calculate ΔQ_{out} at different applied DC powers (Q_{DC}). Finding the linear fit parameters from the plot of ΔQ_{out} vs Q_{DC}, Equation 9 shows us the relationship between applied DC power (Q_{DC}) and the DC power output to the environment (ΔQ_{out}), which cannot be measured directly.

The same equation can be used to find ΔQ_{out} with Q power applied substituting (Q_{pulse}) for Q_{DC}.

$$\Delta Q_{out} = Q_{DC} - (Q_{heater} - Q_{heaterDC}) \qquad\qquad \text{Equation 8}$$

Since $\Delta Q_{out} = m(Q_{DC}) + b \quad$ then $\quad \Delta Q_{out} = m(Q_{\text{pulse}}) + b \qquad$ Equation 9

Equation 10 shows the calculation of $Q_{reaction}$ when operating in power compensation mode where $\Delta Q_{heater} + \Delta Q_{out}$ would equal Q_{pulse} (or Q_{DC}) when $Q_{reaction} = 0$. Equation 11 defines our effective coefficient of performance for the power compensation mode for our isoperibolic calorimeter system.

$$Q_{reaction} = \Delta Q_{heater} - Q_{\text{pulse}} + \Delta Q_{out} \qquad\qquad \text{Equation 10}$$

$$COP = (\Delta Q_{heater} + \Delta Q_{out})/Q_{\text{pulse}} = (\Delta Q_{heater} + m(Q_{pulse}) + b)/Q_{pulse} \qquad \text{Equation 11}$$

Method B
The second method of analyzing the calorimetry is more direct in that instead of calculating the power loss by the calorimeter it determines the amount of heater power compensation (HPC) for different amounts of DC calibration power. In fact, this method is analogous to the traditional isoperibolic calorimeter analysis except that it substitutes heater power compensation for the temperature difference. In order to calculate Q_{reaction} as output power minus input power, Method B compares the heater power compensation (HPC) from DC calibration to that from pulse stimulation. Using this DC calibration the relationship between input power and HPC is determined so that with input pulse power the HPC can be used to back calculate the power from the pulse imparted into the core.

First the linear relationship between HPC and DC power (Q_{DC}) is found by fitting a linear equation to HPC vs Q_{DC} when Q_{DC} is varied across the range of Q_{pulse}. These linear coefficients are then applied to measured Q_{pulse} to calculate HPC(DC), the amount of HPC expected as if the pulse power were DC power. Q_{reaction} is then calculated as shown in Equation 12, where HPC(Q)

is the actual HPC measured when the pulse is applied. Equation 13 is then used to calculate COP.

$$Q_{reaction} = HPC(Q) - HPC(DC)$$ Equation 12

$$COP = Q_{reaction}/Q_{pulse} = (HPC(Q) - HPC(DC))/Q_{pulse}$$ Equation 13

The linear slope coefficient is similar to the value "m" used in Method A. Method A uses the fit to determine the input power lost to the environment and Method B uses the fit to determine the percentage of input power that interacts with the core's heater and thermocouple. Table 3 shows the values for "M", the linear fit coefficient from Method B.

Table 3. List of linear fit coefficients determined and employed in Method B:

Temperature/°C	"M"
150	0.45
200	0.47
250	0.50
300	0.53
350	0.57
400	0.58

For the latter experiments, we concentrated on the tubes with the middle 6 inches of active metal coating, and using the band heaters design. We will also used the low voltage Q pulse, with higher repetition rates, as the reference run unable to produce LENR heat (excess power).

SSS METHOD

In this method the absolute heater power necessary to maintain constant temperature without Q pulses present is not part of the output power calculation. We realize that only a fraction of the heater power may be imparted to the tube because the heater/thermocouple combination has measurable losses to the rest of the calorimeter and to the environment. Instead the temperature controller is instructed to keep the inner block at a constant temperature while low voltage calibration pulses are imparted to the tube and measuring the heater's response at different temperatures. The difference between the heater power with and without the low voltage pulses (LVP) is called P_{drop}. At each temperature, a linear function ($P_{drop} = m*P_{LVP} + b$) is determined. The b offset parameter is always insignificant and is not used in the analysis.

P_{drop}, also called heater power compensation (HPC), is determined for different amounts of LVP calibration power. This method is analogous to the traditional isoperibolic calorimeter analysis except that it substitutes heater power compensation for the temperature difference. In order to calculate $Q_{reaction}$ as output power minus input power, we compare the heater power compensation (HPC) from LVP calibration to that from high voltage pulse (HVP) stimulation. Using this LVP calibration the relationship between input power and HPC is determined so that with input pulse power the HPC can be used to back calculate the power from the pulses

imparted into the tube. Q_{LVP} and Q_{HVP} are the actual Q pulse powers measured when low voltage and high voltage pulses are applied, respectively.

First, the linear relationship between HPC and Q_{LVP} is found by fitting a linear equation to HPC vs Q_{LVP} when Q_{LVP} is varied across the same range of powers as Q_{HVP}. These linear coefficients are then applied to the measured Q_{HVP} to calculate HPC(LVP), the amount of HPC measured at the same temperature and pulse power at low voltage, where no reaction heat is expected. $Q_{reaction}$ is then calculated as shown in Equation 14, where HPC(HVP) is the actual HPC measured when the high voltage pulse is applied. Equation 15 is then used to calculate COP. An alternate calculation is shown in Equation 16. In the latter equation, the COP is calculated as the ratio of the HPC over the Core Q Power at high and low voltage:

$$Q_{reaction} = HPC(HVP) - HPC(LVP) \qquad\qquad \text{Equation 14}$$

$$COP = Q_{reaction}/Q_{LVP} = (HPC(HVP) - HPC(LVP))\ /Q_{LVP} \qquad \text{Equation 15}$$

$$COP = (HPC(HVP)/Q_{HVP})/(HPC(LVP)/Q_{LVP}) \qquad \text{Equation 16}$$

DS METHOD

The DS method employs a model with several components, each representing individual components of the calorimeter. Linkages between these components (and from a component to the reference room temperature) are either conductive or storage. One differential equation (in time) models the heat imparted to the Tube using a function of the difference of the tube and outer block temperature, a function of the tube and inner block temperatures, and divided by the function of the ability of the tube to store heat. Each of these three components have a coefficient that is determined fitting the temperature data to the actual power measured using low voltage pulses as described above. A second equation does the same for the inner block. The model then yields a simple equation for power equal to a coefficient time the difference between the tube and inner block temperatures.

These functions are simple 3-coefficient binomial equations, yielding 15 possible parameters. These parameters are then used to calculate the amount of heat emanating from the tube during an attempt to produce LENR heat. A comparison between the calculated power emanating from the tube during an active run and that from the calibration run at the same temperature and with the same Core Q Power is used to determine the amount, if any, LENR heat was produced. When the DS runs were interrupted to achieve a steady-state, the amount of heater power determined to affect the tube was subtracted from both the input and output powers before calculating COP. This analysis is comparable to but not identical to the calculation used to obtain the results reported in the 2016 report. The computer application MatLab® is used to determine the best fit parameters. A more detailed description of the DS analysis method is given in Appendix B.

RESULTS

A tabulation of all experiments run to date in the IPB calorimeters is shown in Appendix C. Only a fraction of the total number of experiments will be covered in detail.

SSS METHOD RESULTS

The runs detailed in this analysis generally used a 100ns pulse width with similar Q power on the tube at different voltages. Figure 8 shows a plot of the heater power, CoreQPower (the actual power measured as applied across the tube) and the tube temperature all versus elapsed time. We attempted to keep the CoreQPow relatively constant at each temperature.

Figure 9 shows Q voltage and pulse width plotted versus the ratio of HPC/CoreQPow at 250°C to 35°C. This is from an earlier experiment where the pulse width was not held constant. Using the COP as defined in Equation 3, this shows the COP to be much greater at 250°C (1.27) than at 400°C (1.00).

Note that the power compensation/CoreQPow is very dependent on the pulse voltage at 250°C but is essentially unchanged at 400°C. Although the total pulse power from the generator is constant, the pulse power measured at the tube does vary with pulse voltage, as shown in Figure 8, even though we attempted to keep Core Q Power constant by also varying the repetition rate and/or pulse width. Still, the magnitude of the power compensation is a greater percentage of the pulse power at 350 v than at 35 v. Calculations show that $Q_{reaction}$ is greater at 350 v than at 35 v. Table 4 summarizes the COP results from recent SSS runs.
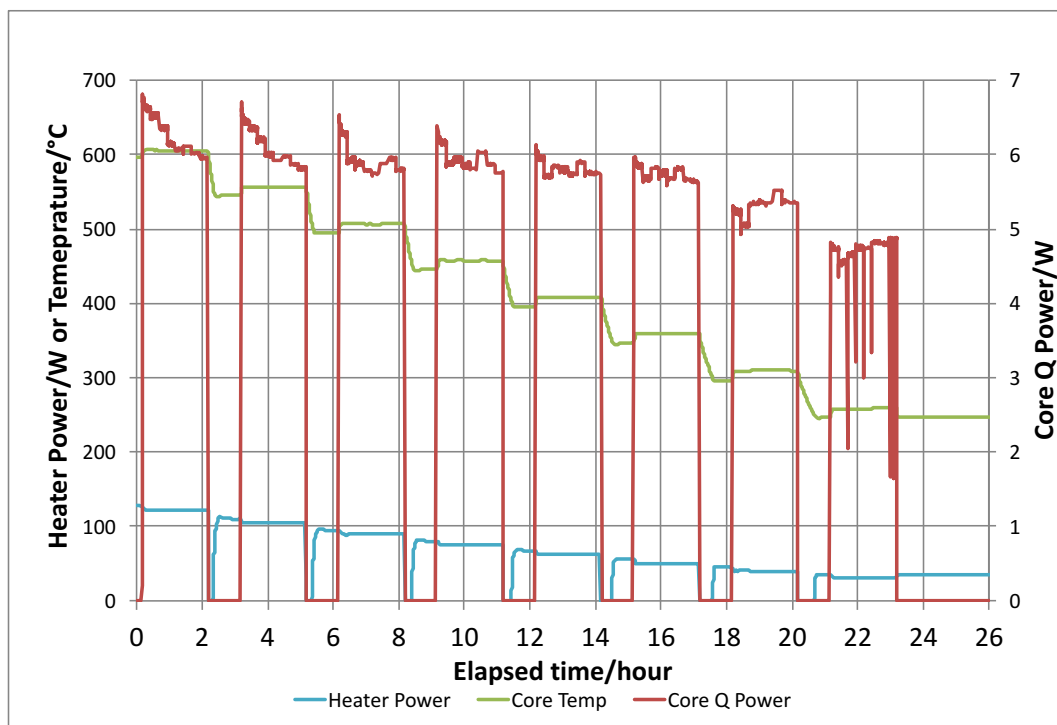

Figure 8. Plot of tube Q pulse power, heater power, and tube temperature from 250 to 600°C.
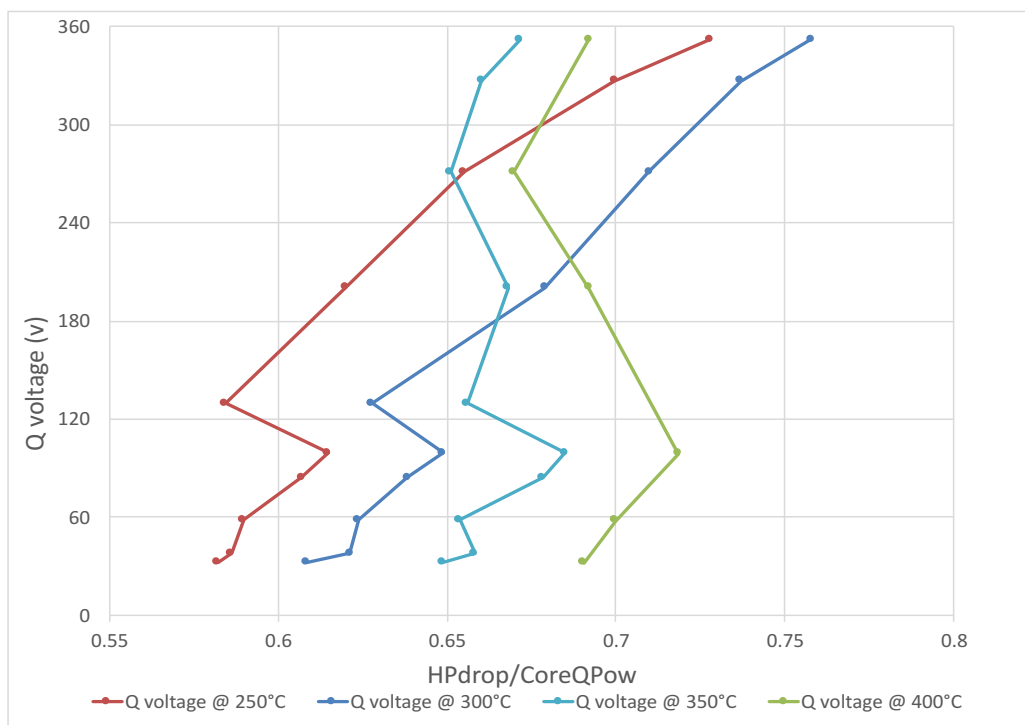
Figure 9. Plot of Q voltage and pulse width versus heater power compensation/CoreQPow from 250 to 350°C.

Table 4. Summary of COP calculations from steady-state stimulation runs:

Temperature/°C	COP : IPB2-33	COP: IPB2-74	COP IPB1-45	COP IPB1-48
250	1.27	1.14		
275	1.4	1.15	1.11	1.13
300	1.25	1.13	1.11	
325	1.26	1.09	1.08	1.27
350	1.05	.94		
400	1.00	.89		

DS METHOD RESULTS

The DS method employed in the latter half of 2017 calculated two different COP results. The first was the average COP over the complete stimulation run. The other result calculated instantaneous COP, especially at the point of greatest stimulation amplitude. (See the description of the dynamic stimulation method in the Operation section above and in Appendix C). Two tubes showed particularly good COP's both in the average and instantaneous calculations. Table 5 shows a representative example of some of the better average COP's achieved in latter experiments. We also found that the best COP's were achieved between 250 and 350°C, confirming the results that were reported earlier. The result in the last row was from figure 10

(b). The results in the last column were calculated by subtracting the heater power affecting the tube from both the input and output powers allowing for direct comparison to last year's results.

Table 5. Average COP's from some DS runs using 100ns pulse width during 2017

Temperature/°C	$Q_{REACTION}$/Watts Above input power	COP using DS method	COP using legacy method
300	3.62	1.25	1.56
340	2.71	1.16	1.37
300	3.59	1.26	1.55
340	3.22	1.19	1.43
300	3.90	1.27	1.62
340	3.58	1.21	1.44
300	4.91	1.31	1.56
340	5.29	1.27	1.52
300	4.99	1.31	1.58
340	5.35	1.27	1.53
300	4.85	1.31	1.58

Figure 10a shows an example of the instantaneous COP calculated using the DS analysis method from a recent run. To prove that this COP is stable the stimulation parameters were held constant for 4 hours. This latter result is shown in Figure 10b. Although the numbers presented seem no better than last year's, when the method similar to that used last year is used to calculate the COP, we get significantly larger results shown in the right-most column of Table 5. It is also important to note that the absolute LENR powers ($Q_{reaction}$) are significantly larger.

The active tube, whose results are presented in Figure 10 and was removed from service at BEC during December 2017, was placed in service at SRI in a different reactor during April 2018 and showed similar results. These latter plots are shown in Figure 11. Table 6 summarizes the results from some runs during the first half of 2018.

In addition to the plasma sprayed tubes, two tubes were constructed from 5μm thick electroformed Ni mesh which had 10μm of PdHx electrodeposited onto it using the procedure of Mosier-Boss. The second of these tubes showed a very good facility to absorb hydrogen reversibly and is still undergoing pulse stimulation and calorimetric tests.
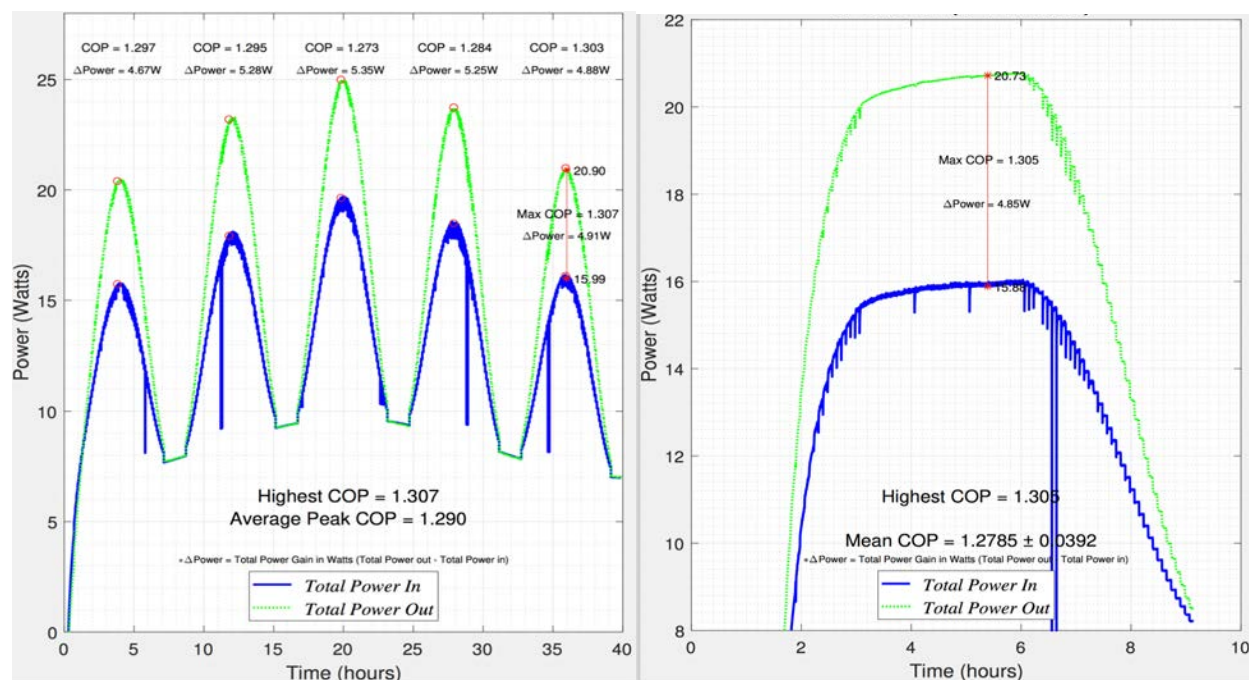
Figure 10. (a) Instantaneous COP during DS run, (b) COP during 4 hours at maximum stimulation.
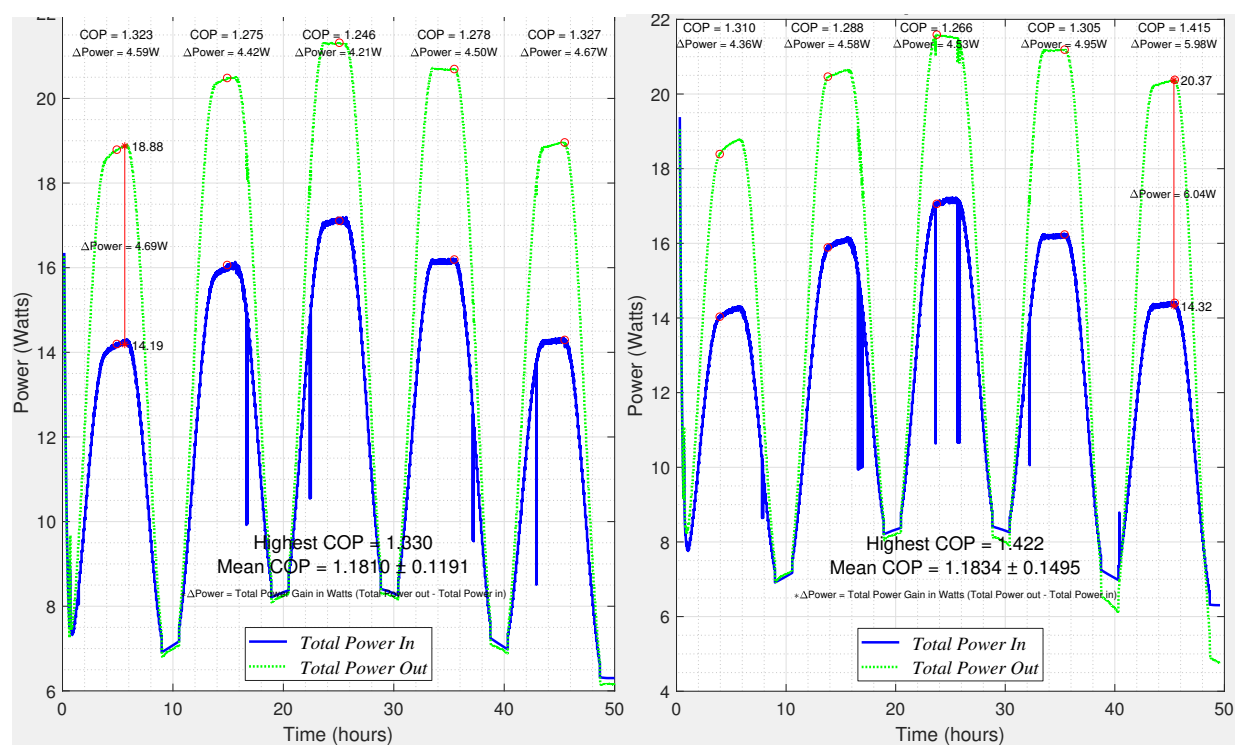

Figure 11. COP during two different DS runs with 2 hours at maximum stimulation.

Table 6. Average COP's from some DS runs using various pulse widths during early 2018

Temperature/°C	$Q_{REACTION}$/Watts Above input power	COP using DS method	COP using legacy method
300	4.59	1.32	1.59
340	4.21	1.28	1.53
300	4.67	1.33	1.6
300	4.36	1.31	1.58
340	4.53	1.27	1.53
300	5.98	1.41	1.62

CONCLUSIONS

Low energy nuclear reactions (LENR) can produce thermal power when Ni, and other metal, coated tubes are stimulated using fast rise-time pulses. These experiments operated in H_2 or He gas from 200°C – 600°C. The exact same procedure was performed in each gas. Comparative thermal measurements were performed between heater-only power and heater and pulse power.

These runs were performed in isoperibolic calorimeters operated in power compensation mode, where the heater adjusts its power to keep the inner and outer temperature-difference constant. Over 100 runs were performed on 34 different Ni-coated tubes during the first seven months of 2018. Additional tubes were also tested for other experimental purposes. 2017 was spent optimizing tube design, stimulation protocols, calorimeter design, and calorimetric analysis methods. The accuracy and precision of this year's best results have been considerably better than the prior year's best results.

The most recent methodology has required design compromises that caused the capture efficiency of the heater power entering the calorimeter to be reduced. Advances in tube designs have allowed essentially all of the stimulation power entering the calorimeter to be captured and measured accurately. Also, a significant amount of the stimulation power generated at the power supply is not imparted to the calorimeter. It is expected that via straightforward engineering design advances we will be able to minimize the heat not imparted to the tube by the heater and also to minimize the electrical losses seen in the production of the Q pulse. Although the raw numbers presented seem no better than last year's, when the method similar to that used last year is used to calculate the COP, we get significantly larger results than those measured last year. It is also important to note that the absolute LENR powers ($Q_{reaction}$) are significantly larger.

Correlation of different fabrication materials and methods as well as various electronic measurements with measured COP have shown which methods are more successful and allow us to design reactor tubes more likely to yield high COP. These results are given in the Confidential Client Private Addendum.

In summary, we feel that it is obvious that important progress has been made in 2017. We also feel that continued progress was made in 2018. We feel that more progress can be made with

even greater expanded effort and focus on increasing the COP and optimizing the calorimeter design.

ACKNOWLEDGEMENTS

APPENDIX A: IPB TUBE DESIGNS TESTED

reactor + tube	dates	comments	properties
Ipb1-26	8/18/2016– 9/26/2016	Died @ 400°C	Ni
Ipb1-29	9/29/2016– 10/31/2016		Ni-Pd
Ipb1-30	11/1/2016– 3/2/2017		Ni-Pd
Ipb1-40	3/6/2017– 4/5/2017		Ni-Pd
Ipb1-41	4/5/2017 – 6/29/2017	Run at both BEC & SRI	Ni-Pd
SRI-ipb1-48	6/29/2017 – 7/25/2017	good	Ni-Pd
SRI-ipb1-45	7/25/2017 – 8/15/2017	good	Ni-Pd
SRI -ipb1-43	8/16/2017 – 10/17/2017	good	Ni-Pd
SRI -ipb1-54	10/17/2017 – 10/27/2017	good	Ni-tube(he)
SRI -ipb1-66	10/27/2017 – 11/06/2017	in-service	Ni-ceramic-tube
SRI -ipb1-66	11/06/2017 – 11/10/2017	changed probe	Ni-ceramic-tube
SRI -ipb1-66	11/10/2017 –-12/15/2017	sanded	Ni-ceramic-tube
SRI-IPB1-94	12/15/2017---1/18/2018		Ni-ceramic-tube
SRI-IPB1-98	1/18/2018---3/9/2018		Ni-ceramic-tube
SRI-IPB1-90	3/9/2018—3/31/2018		Ni-ceramic-tube
SRI-IPB1-107	4/3/2018—5/11/2018		Ni-ceramic-tube
SRI-IPB1-73	5/11/2018—	Same as 72 tube	Ni-ceramic-tube
Ipb2-22	3/30/2016 – 6/29/2016	good	Ni-Pd
Ipb2-25	6/29/2016 – 7/6/2016	good?	Ni-Pd
Ipb2-23	7/6/2016 – 7/22/2016	good?	Ni-Pd
Ipb2-20	08/19/2016 – 8/22/2016	good?	Ni-Pd
SRI -ipb2-27	09/26/2016 – 2/10/2017	good?	Ni-Pd
SRI -ipb2-33	02/10/2016 – 9/14/2017	good?	Ni-Pd
SRI -ipb2-55	09/15/2017- 10/19/2017	good?	Ni-Pd
SRI -ipb2-83	10/19/2017 – 10/27/2017	good	Ni-Pd-Cu-ends
SRI -ipb2-67	10/27/2017 – 11/7/2017	good	Ni-ceramic-tube
SRI -ipb2-67	11/7/2017 – 11/10/2017	changed probe	Ni-ceramic-tube
SRI -ipb2-74	11/10/2017 –12/15/2017	good	Ni-ceramic-tube
SRI -ipb2-74	12/15/2017 –1/4/2018	good	Ni-ceramic-tube
SRI-IPB1-89	1/4/2018---3/15/2018	good	Ni-ceramic-tube
SRI-IPB1-92	3/15/2018---4/19/2018	good	Ni-ceramic-tube
SRI-IPB1-92	4/19/2018---Present	Retest IPB35-72	Ni return line
ipb3-43	5/15/2017 - 8/1/2017	good	Ni-Pd
ipb3-39	8/3/2017 - 8/9/2017	good	PD-RH foil
ipb3-56	8/9/2017 – 8/28/2017	bent	Ni-Pd
Ipb35-51	8/28/2017 – 10/3/2017	bend	Ni-tube

reactor + tube	dates	comments	properties
Ipb35-62	10/3/2017 – 10/26/2017	good	Ni-Pd-Cu-ends
Ipb35-72	10/26/2017-11/06/2017	good	Ni-ceramic-tube
Ipb35-72	11/6/2017---2/6/2018	changed probe	Ni return line
Ipb35-87	2/6/2018---2/26/2018		Ni
Ipb35-88	4/13/2018---4/30/2018		Ni
Ipb35-110	5/3/2018---5/28/2018		Ni
Ipb35-95	5/28/2018---7/9/2018		Ni
Ipb35-123	7/11/2018---		Ni
ipb41-44	6/12/2017 - 7/10/2017	ridged	Ni-Pd
ipb41-50	7/10/2017 - 7/24/2017	good	Ni-
ipb41-53	7/24/2017 - 8/10/2017	rippled	Ni-
ipb42-52	8/10/2017 - 8/14/2017	good	Ni-
Ipb43-14	08/16/2017 – 8/25/2017	good	Ni-
Ipb43-14	08/26/2017 – 8/31/2017	good	Ni-tube-NP-11nf
Ipb43-14	09/04/2017 –	good	Ni-tube-NP-22nf
Ipb43-14	09/07/2017 – 9/25/2017	bent & peeled	Ni-tube-NP-32nf
Ipb45-58	09/26/2017---11/03/2017	good	Ni-ceramic-tube
Ipb45-58	11/03/2017---12/13/2017	changed probe	Ni-ceramic-tube
IPB45-86	12/14/2017---12/19/2017	Good?	Ni-Pd
IPB45-64	12/20/2017---1/4/2018		Ni mesh
Ipb45-63	1/4/2018---1/23/2018	2nd gen Q board	Ni-electroform-mesh
IPB45-97	1/23/2018---2/7/2018	2nd gen Q board	Ni
IPB45-85	2/8/2018---3/2/2018	Diff Probes	Ni-Pd
IPB45-105	3/2/2018---3/30/2018	Diff Probes	Ni
IPB45-98	3/30/2018---4/2/2018		NiMH electrode
IPB45-109	4/2/2018---4/17/2018		Ni
IPB45-111	4/17/2018---5/25/2018	Different code versions	Ni-Pd
IPB45-114	5/25/2018---7/6/2018	Code 1.8.13	Ni
IPB45-117	7/6/2018---7/25/2018		Ni
PB45-122	7-25/2018---	Measured H2 loading	Ni mesh + Pd codep

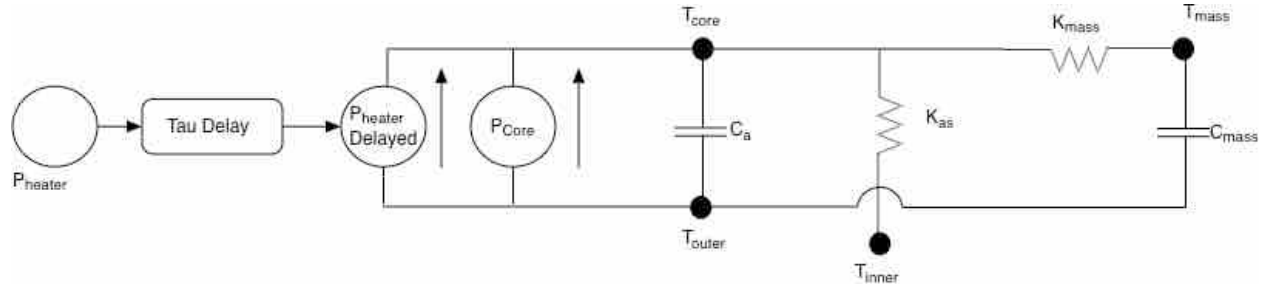## APPENDIX B: DS ANALYSIS METHOD DETAILED DESCRIPTION

Figure B.1 Equivalent circuit representation of the IPB calorimeter's thermal conduction and storage

Figure B.1 gives a representation of the thermal conduction and loads of the IPB reactor using an electronic equivalent circuit. Each of the thermal components are represented by one of the electronic components. Every important thermal component has a thermocouple as part of it. The resistance to thermal conduction between two thermal components are represented by a resistor. Storage in the thermal mass of a component is represented by a capacitor. Heat sources are represented as power supplies.

Starting from the left side of the figure, the heater power is delayed in reaching the tube by the thermal mass of the inner block. This thermal time constant is represented by tau. This "$P_{heater,delayed}$" is easily handled in the analysis by simply using the measured heater power from an earlier time in the data file. The Q pulse stimulation power is (P_{tube}) is closely couple to the tube and does not require a temporal delay. The individual thermal components are labeled T_{tube}, T_{mass}, T_{inner} and T_{outer}. Each of these components has a thermocouple associated with it. T_{mass} is associated with the thermocouple in the inner tube positioned axially near one end of the inner block, as described in Figure 3. T_{inner} is measured via the thermocouple placed between the band heater and the inner block. T_{tube} is measured in the annular cavity inside the tube. T_{outer} is measured by a thermocouple inserted into the outer block, kept at constant temperature via cooling water.

The ultimate goal of this analysis is to determine the appropriate coefficient equations, that when operated on the measured temperatures will yield the amount of power emanating from the tube. This is done by first setting up differential equations in time for changes in T_{tube} and T_{mass}.

$$dT_{tube}/dt = (1/c)\{\alpha P_{heater,delayed} + P_{tube} - k_{as}(T_{tube} - T_{inner}) - k_{mass}(T_{tube} - T_{mass})\} \qquad \text{Equation B1}$$

$$dT_{mass}/dt = (k_{mass}/c_{mass})(T_{tube} - T_{mass}) \qquad \text{Equation B2}$$

where c is a representation of both c_a and c_{mass}. Input and output powers are represented by:

$$P_{in} = \alpha P_{heater,delayed} + P_{tube} \qquad \text{Equation B3}$$

$$P_{out} = k_{as}(T_{tube} - T_{inner}) \qquad \text{Equation B4}$$

The coefficient k_{as} is actually a binomial equation, which is found using the heater only runs and the runs with low Q voltage where no LENR power is expected. This coefficient is then used to calculate the output power present during a high Q voltage run using Equation B4 using T_{tube} and T_{inner} measured during that run. Similarly, Equation B3 is used to calculate the input power present during the high Q voltage run. COP is found by dividing the calculated P_{out} by the calculated P_{in}.

In order to validate the model P_{stored} is calculated using Equation B5:

$$P_{stored} = c(dT_{tube}/dt) + c_{mass}(dT_{mass}/dt) \hspace{4cm} \text{Equation B5}$$

Matlab® is used to find all of the coefficient binomial equations which yield the best fit to the measured data. Then Equations B3 and B4 are used to calculate COP's during the high Q voltage run as shown in Figure 10.